I&EC research
Industrial & Engineering Chemistry Research

pubs.acs.org/IECR
Article

Enzyme Immobilization on Stimuli-Responsive Hydrogels - Part A. Influence of Carrier Properties on Immobilization Efficiency and Catalytic Performance

Published as part of Industrial & Engineering Chemistry Research special issue "Smart Reactors - Towards Adaptive, Resilient, and Autonomous Process Systems".

Kayla Reata Dittmer, Kathrin Marina Eckert, Sherliana Setiawan, Patrick André Kißling, Daniel Ohde, Irina Smirnova, and Andreas Liese*

Cite This: https://doi.org/10.1021/acs.iecr.6c00961

ABSTRACT: Enzyme immobilization on stimuli-responsive hydrogels provides a strategy to control biocatalytic activity under fluctuating process conditions. In this study, the immobilization of formate dehydrogenase on three hydrogel carriers is investigated: pH-responsive poly(2-hydroxyethyl methacrylate-*co*-itaconic acid), temperature-responsive poly(*N*-isopropylacrylamide), and dual-responsive poly(*N*-isopropylacrylamide-*co*-itaconic acid). The hydrogels were characterized in terms of swelling behavior, mechanical properties, and morphology, confirming the responsiveness of these materials. Subsequently, the immobilization performance was evaluated across two carrier geometries (monoliths and particles) and two immobilization techniques (adsorption and covalent binding). The polymer chemistry was identified as the dominant factor controlling enzyme loading density, with the dual-responsive formulation achieving the highest loading despite moderate immobilization yields. These responsive hydrogels demonstrate strong potential as smart enzyme carriers for biocatalytic applications, particularly in continuous-flow reactor designs where improved substrate availability and increased convection can mitigate diffusion limitations and fully exploit both the catalytic performance and stimuli-responsive properties of the immobilized enzyme systems.

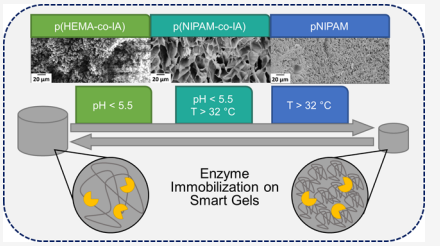

INTRODUCTION

The sensitivity of biocatalysts to environmental fluctuations in reaction conditions is a major challenge for their practical application. Consequently, immobilization techniques and materials have become a central focus of current research, aiming to enhance the stability and performance of biocatalysts.[1,2] An industrially relevant sensitive enzyme was chosen in this work as a model biocatalyst. Formate dehydrogenase (FDH) from *Candida boidinii* catalyzes the reduction of the cofactor NAD^+ to NADH with formate as a hydrogen source, generating CO_2 as a side product. Under certain process conditions, particularly in continuous operation, immobilization can enhance enzyme stability and retention.[3] In nature, cofactor regeneration typically occurs naturally through cellular metabolic cycles. *In vitro* biocatalyzed hydrogenations with NAD(H)-dependent biotransformations usually require the supply of low (catalytic) cofactor concentrations coupled with auxiliary enzymes or electrochemical methods to sustain turnover. Without regeneration, the reaction would indeed consume NADH stoichiometrically, which is economically prohibitive for industrial biotransformations given cofactor cost; hence, cofactor regeneration is a central aspect of this study.[4]

In this context, stimuli-responsive materials have emerged over the past decades as alternative enzyme carriers.

Stimuli-responsive gels, capable of reversible swelling or shrinkage in response to external triggers, have found applications across various fields such as such as flow-regulation,[5] drug delivery,[6] and sensing and actuation.[7,8] Depending on the choice of monomers, these materials can be designed to respond to various triggers, such as temperature,[9] pH,[10] light,[11] or magnetic and electric fields.[6] Moreover, different fabrication strategies enable the preparation of a wide range of material formats, including monoliths, beads, films, and polymer brushes, as well as tailored three-dimensional architectures via additive manufacturing. Their porous network structure provides a high surface area, which is particularly advantageous for enzyme immobilization.[12] Previous studies have demonstrated the utility of stimuli-

Received: March 4, 2026
Revised: April 30, 2026
Accepted: May 15, 2026

https://doi.org/10.1021/acs.iecr.6c00961
Ind. Eng. Chem. Res. XXXX, XXX, XXX−XXX

responsive gels as enzyme carriers, reporting successful immobilization of ribonuclease A,[13] alkaline phosphatase,[14] or lipase B.[15] Beyond these studies of their performance as enzyme carriers, recent research has examined the switchability of biocatalytic activity,[14,16−18] or the morphology of the carriers[11,15] in various systems. While the dependence of enzymatic activity on pH and temperature is well established, González-Sáiz and Pizarro[14] demonstrated that pH-responsive acrylamide gels can be employed to actively control the activity of alkaline phosphatase under varying pH conditions. In line with the approach of Nagel et al.,[17] Dübner et al.[11] reported switchable microperoxidase activity using light-responsive polymer brushes, resulting in a larger surface area for enzyme carriers compared to monolithic gels. Extending these strategies toward mophologies with enhanced surface area, Eixenberger et al.[15] employed polyamide-based additive manufactured lattice structures (AMLS), designed to improve reactor flow properties. These scaffolds were grafted with poly(acrylic acid) (PAA) to serve as enzyme carriers, achieving a notably increased enzyme loading on the carrier surfaces following polymer grafting. Although the polymers exhibited pH responsiveness, the response time was slow, spanning hours, and the carrier's recyclability was found to be limited. In addition to the earlier findings of González-Sáiz and Pizarro,[14] both Dübner et al.[11] and Eixenberger et al.[15] extended the approach of responsive carriers to enhanced morphologies, with Dübner et al. utilizing polymer brushes and Eixenberger et al. additive-manufactured lattice structures.

In this study, we investigate responsive materials based on *N*-isopropylacrylamide (NIPAM) and itaconic acid (IA), with temperature- and pH-responsive matrices resulting from the NIPAM and IA monomeric units, respectively. While the pH-responsivity of the gels depends on the ionization of the carboxylic acid groups from itaconic acid,[10] the temperature-responsivity is governed by the lower critical solution temperature (LCST) of poly(*N*-isopropylacrylamide) (pNIPAM).[16,19] These characteristics cause gel shrinkage at low pH in IA-containing gels and at elevated temperatures in pNIPAM-containing gels. The synthesis of copolymers from both monomers results in dual responsivity, with thermoresponsiveness arising from the NIPAM units and pH-responsiveness from the incorporation of itaconic acid. In previous studies, distinct polymers have been employed as either single-responsive[15,20] or even dual-responsive[16,21] matrices for enzyme immobilization. In the work of Koenig et al.[16] pH-sensitive brushes composed of poly(2-vinylpyridine) (P2VP) or poly(acrylic acid) (PAA) were coated with pNIPAM for the purpose of immobilizing glucose oxidase. The P2VP and PAA brushes contributed to pH responsiveness, while pNIPAM provided temperature sensitivity in the gel matrix. It was found that the enzymes adsorbed more effectively to PAA at pH 5, but exhibited lower specific activity compared to P2VP. The pNIPAM coating reduced the total amount of adsorbed enzyme compared to the single-component brushes. This difference was attributed to the distinct charge state and hydrogen-bonding capability of the PAA and P2VP brushes at the working pH, which govern specific electrostatic interactions with glucose oxidase. Nevertheless, a temperature-dependent switch in enzyme activity was observed at pH 4, with an active state at 20 °C and an inactive state at 40 °C. An overview on current research in enzyme immobilization on responsive materials is provided by Claßen et al.,[22] Nöth et al.,[23] and Dubey et al.[24]

Building on these foundational studies, this work focuses on investigating pH-, temperature-, and dual-responsive polymer gels as carrier matrices for the immobilization of FDH. The catalytic performance of the immobilized enzyme based on distinct immobilization techniques and the stimulus-responsiveness of the gel matrices are evaluated in detail. The overall aim of this study is to demonstrate the applicability of responsive polymer systems as smart carriers for sensitive *in vitro* biocatalysts such as FDH in economically relevant biocatalytic applications. The UNU Hub at TUHH advances the United Nations' sustainability objectives, especially SDG 12 on Responsible Consumption and Production and SDG 9 on Industry, Innovation, and Infrastructure by developing bioprocess engineering methods that are cleaner and more sustainable.

EXPERIMENTAL METHODS

Materials

NIPAM (≥ 98%) and *N*-hydroxysuccinimide (NHS, 98%) were obtained from Abcr GmbH (Karlsruhe, Germany). 2-hydroxyethyl methacrylate (HEMA, 97%) and *N*,*N*′-Methylenebis(acrylamide) (MBA, 99%) were purchased from Merck Sigma-Aldrich (St. Louis, MO, USA). Sodium metabisulfite (NaDS, ≥ 97%) was supplied by Honeywell Fluka (Buchs, Switzerland), and FDH (2 U/mg) by Megazyme Ltd. (Bray, Ireland).

NAD^+ (≥ 95% purity), sodium formate (HCOONa, ≥ 99%), RotiQuant Solution (5x conc.), bovine serum albumin (BSA, ≥ 98%), ortho-phosphoric acid (≥ 85 wt%), IA (≥ 98%), silica gel orange (2−5 mm, with indicator, pearl shaped), ammonium persulfate (APS, ≥ 98%), monopotassium phosphate (KH_2PO_4, ≥ 98%), dipotassium phosphate (K_2HPO_4, ≥ 98%), 2-morpholinoethanesulfonic acid (MES; ≥ 99%) and 1-ethyl-3-(3-(dimethylamino)propyl)-carbodiimide (EDC, ≥ 99%), were all purchased from Carl Roth GmbH + Co. KG (Karlsruhe, Germany).

Gaseous nitrogen (99.99%) was supplied by Westfalen AG (Münster, Germany) and liquid nitrogen (99.999%) by Linde GmbH (Pullach, Germany).

Hydrogel Synthesis and Characterization

This study provides a comparison of material properties and the application as an enzyme support of a pH-responsive, a temperature-responsive, and a dual (pH and temperature)-responsive hydrogel: p(HEMA-*co*-IA), pNIPAM, and p(NIPAM-*co*-IA), respectively. In the copolymeric formulations, the monomer composition consisted of 88 mol% of the primary monomer (HEMA or NIPAM), 10 mol% IA, and 2 mol% MBA as cross-linker, all relative to the total monomer content. For the homopolymeric pNIPAM formulation, IA was omitted, resulting in 98 mol% NIPAM and 2 mol% MBA. The responsive hydrogels were synthesized by radical polymerization, according to the formulation in Table 1.

Table 1. Hydrogel Synthesis: p(HEMA-*co*-IA), p(NIPAM-*co*-IA), pNIPAM

	pH responsive	dual responsive	temperature responsive
Chemicals	p(HEMA-*co*-IA)	p(NIPAM-*co*-IA)	pNIPAM
HEMA (mmol)	27.66	-	-
NIPAM (mmol)	-	27.66	30.94
IA (mmol)	3.08	3.08	-
MBA (mmol)	0.62	0.62	0.62
APS (mmol)	0.31	0.31	0.31
NaDS (mmol)	0.20	0.20	0.20
Water (g)	20.00	20.00	20.00

https://doi.org/10.1021/acs.iecr.6c00961
Ind. Eng. Chem. Res. XXXX, XXX, XXX−XXX

For the polymerization, the monomers and cross-linker were dissolved in deionized water and degassed with nitrogen for 30 min. Subsequently, 0.07 g of APS and 0.058 g of NaDS were dissolved in 1 mL deionized water and added to the mixture. In order to determine the effect of hydrogel size on the immobilization parameters, two diameters were formulated. The monolith hydrogels were cast in 10 mL B. Braun SE (Melsungen, Germany) syringe syringes with an inner diameter of 1.0 cm and the particle hydrogels were cast in 1 mL B. Braun SE (Melsungen, Germany) syringes with a 0.5 cm inner diameter. The gelation process took 24−48 h. After the completion of the gelation process, the hydrogels were removed from the syringes and cut into monoliths of 1 cm in length or particles of 0.5 cm length. Finally, the hydrogels were washed by immersion in deionized water for 72 h, with the water replaced daily, to ensure the removal of unreacted components.

After synthesis, the gels were characterized by comparing the swelling behavior and mechanical properties of the hydrogels. The degree of swelling (*Dos*) for the different formulations was calculated using eq 1 as the ratio of the mass of equilibrated hydrogels ($m_{equilibrated\ gel}$) to the dry mass of the polymer ($m_{dried\ polymer}$). The hydrogels were equilibrated in deionized water for 24 h at 25 °C using an OLS 200 water bath (Grant Instruments, Cambridge, United Kingdom). The dry mass was obtained by drying the wet gels in a vacuum oven (VT 6060 M-BL, Thermo Scientific; Waltham, MA, USA) at 40 °C for 48 h.

$$Dos = \frac{m_{\text{equilibrated gel}}}{m_{\text{dried polymer}}} \tag{1}$$

The relative swelling was analyzed with respect to both temperature- and pH-responsiveness. For both analyses, the hydrogel monoliths were first equilibrated in deionized water for 24 h at 25 °C using a water bath, following the procedure for the degree of swelling analysis.

For the pH-responsive swelling analysis, the hydrogels were transferred into a 50 mM potassium phosphate buffer solution (pH 8, state *I*), shaken for 24 h and then equilibrated for an additional 48 h without agitation. The weight of the hydrogels after equilibration were recorded using an analytical balance. Subsequently, the hydrogels were submerged stepwise in 50 mM potassium phosphate buffer solution of pH 7, pH 6 and finally pH 4 (state *II*), with the same equilibration and measurement procedures repeated at each step. For the pH 4 buffer, the pH was lowered by the addition of 85 wt% ortho-phosphoric acid.

Temperature-induced swelling was analyzed by measuring the swelling behavior at 25 °C (state *I*) and 40 °C (state *II*) in deionized water, without a stepwise temperature change. The relative swelling *S* from state *I* to state *II* was calculated using eq 2, respectively.

$$S = \frac{m_I}{m_{II}} \tag{2}$$

In addition, the elastic modulus was determined using uniaxial compression (Universalprüfmaschine Z1474, nominal force: 2.5 kN; ZwickRoell GmbH & Co. KG; Ulm, Germany) under ambient conditions. The analysis was performed using a flat cylindrical stamp with a diameter of 40 mm, exceeding the sample dimensions to ensure complete contact throughout the measurement. The stamp was lowered toward the hydrogel until a minimal contact force of 0.02 N was detected, marking the starting point of the test. Compression was applied at a constant rate of 50 mm/min. The measurement was terminated upon reaching either 75% strain or the maximum force capacity of the load cell (50 N, ZwickRoell GmbH & Co. KG, Xforce HP; Ulm, Germany). Force and displacement data were continuously recorded throughout the test duration. The elastic modulus E_C was determined from the linear region of the force-deformation curve corresponding to the elastic deformation. Using the slope of the elastic deformation Δ and the cross-sectional area of the hydrogels *A*, the elastic modulus was calculated according to eq 3.

$$E_C = \frac{\Delta}{A} \tag{3}$$

Enzyme Immobilization

In this study, we systematically compared two gel geometries (monoliths and particles), three immobilization approaches (adsorptive and covalent with different incubation times), and four biocatalytic characterization parameters (immobilization yield, enzyme loading, residual activity, and leaching). In addition to adsorption and covalent binding, enzyme entrapment was investigated. However, this approach resulted in heterogeneous gels during synthesis and was therefore not pursued further in this study. An overview of the experimental design is provided in Table 2. If not stated otherwise, 50 mM potassium phosphate buffer (pH 8) was used.

Table 2. Overview of Experimental Parameters Investigated for Enzyme Immobilization and the Analysis Methods

Process Parameters	
Monomer(s)	HEMA-*co*-IA
	NIPAM-*co*-IA
	NIPAM
Hydrogel Geometry	Monoliths (Ø 10 × 10 mm)
	Particles (Ø 5 × 5 mm)
Immobilization Method	Adsorption (24 h)
	Covalent binding (3 h)
	Covalent binding (24 h)
Characterization Parameters	
Gel Characterization	Hydrogel Swelling
	Mechanical Stability
Enzymatic Performance	Immobilization yield
	Enzyme Loading
	Enzyme Activity
	Enzyme Leaching

Adsorptive enzyme immobilization was carried out by incubating the hydrogels in an enzyme solution containing 100 μ L FDH (2 U/mg or 75 U/mL) and 14.9 mL buffer solution, resulting in a final enzyme concentration of 0.5 U/mL. The masses of carriers used in the experiments were 3.5 g for p(HEMA-*co*-IA), 11.1 g for p(NIPAM-*co*-IA), 5.2 g for pNIPAM, and 2.0 g for silica. The differing carrier masses reflect variations in hydrogel swelling degree, while the dry mass of the hydrogels was maintained approximately constant (∼0.1 g). The incubation was carried out at 4 °C for 24 h using an overhead shaker to ensure adequate mixing. Aliquots of 150 μ L were taken from the enzyme solution at the start of the incubation and then after 1, 2, 4, 6, and 24 h to monitor the enzyme immobilization process. To ensure repeatability, each immobilization (n = 3) was analyzed three times. The protein concentration was determined using RotiQuant Solution for the Bradford assay.[25] 200 μ L of RotiQuant Solution (1x conc.) was mixed with 50 μ L sample for 5 min at 25 °C in the dark in a T00 PRO microplate reader (Tecan Group Ltd.; Männedorf, Switzerland). The 595/450 nm absorbance ratio was employed for quantification, with calibration performed using bovine serum albumin across a concentration range of 0−200 μ g/mL. As a perspective for future immobilization characterization, a recent study has reported a method for enzyme analysis employing a benchtop NMR device.[26] For the covalent binding of the enzymes to the hydrogels, the EDC/NHS covalent binding method from Wang et al.[27] was adapted to hydrogel carriers. In short, the prepared hydrogels were equilibrated in distilled water for 24 h before the activation process. The hydrogels were first reacted with 52 mM EDC in the presence of 86.8 mM NHS to form a semistable amine-reactive NHS-ester. EDC activates carboxyl groups into reactive intermediates that are stabilized by NHS and subsequently react with amine groups on the enzyme to form stable amide linkages. This process was performed at 25 °C for 3 h. A total of 15 mL of 100 mM MES

https://doi.org/10.1021/acs.iecr.6c00961
Ind. Eng. Chem. Res. XXXX, XXX, XXX−XXX

buffer pH 5 was used in this coupling process to provide an acidic environment. The hydrogels were rinsed with 10 mL buffer to wash off the excess EDC and NHS. Once the hydrogels were functionalized, the hydrogels were submerged in the enzyme solution as described previously for the adsorption. Silica is a mesoporous and inert material that is widely used in enzyme immobilization applications.[28] Silica gels are used as nonresponsive support material and for this specific material, the immobilization was only performed by adsorption since there were no functional groups compatible with the EDC/NHS functionalization method. Silica beads were presorted using a 4 mm sieve to yield particles with diameters approximately matching those of the hydrogel particles (0.4−0.5 cm diameter). The FDH was immobilized on the silica beads by adsorption using the same procedure as for the hydrogels, with the alteration that the gels were first placed above water level in a closed water bath at 40 °C overnight for vapor adsorption. This vapor-based prewetting was necessary because immediate immersion of dry silica in liquid caused the beads to fracture due to capillary forces generated by rapid water intrusion into the mesopores.

FDH Activity Assay

The activity of immobilized enzymes was assessed using an enzyme activity assay for FDH. One unit of enzyme activity was defined as the quantity of enzyme catalyzing the formation of 1 μ mol NADH per minute. Each immobilizate was added to a substrate solution containing 200 mM sodium formate and 1 mM NAD^+ in 50 mM potassium phosphate buffer with pH 8. Aliquots of 150 μ L of the reaction solution were taken at the following time intervals: every 10 min for the first hour, every 30 min for the second hour, and every hour until 5 h of reaction was completed. FDH activity was measured by measuring the NADH absorbance at 340 nm using the 200 PRO microplate reader (Tecan Group Ltd.; Männedorf, Switzerland). The NADH concentration c was determined from the absorbance A, the liquid path length l, and the extinction coefficient ε of NADH at 340 nm using the Lambert−Beer Law as seen in eq 4.

$$c = \frac{A}{\varepsilon l} \tag{4}$$

The absorbance in microplates is measured vertically through the well, and factors such as sample volume, meniscus shape, and well geometry can influence this value and consequently the absorbance values. To determine the liquid path length of 100 μ L in the well plate, a method was used to standardize absorbance readings obtained from microplate measurements, aligning them with those measured in standard cuvettes with a fixed path length of 1 cm. The liquid path length for 100 μ L reaction solution inside a well was calculated using a ratio of the difference in absorbance at 975 and 900 nm for the well plate to that in a standard 1 cm cuvette as described in[29] (eq 5).

$$l = \frac{A_{975(\text{well})} - A_{900(\text{well})}}{A_{975(\text{cuvette})} - A_{900(\text{cuvette})}} \times 10\ \text{mm} \tag{5}$$

Immobilization Characterization

To characterize the immobilization of FDH on the hydrogels, four parameters were evaluated: immobilization yield, enzyme loading, activity yield, and enzyme leaching.

The immobilization yield (Y_{immo}) was defined as the percentage of enzyme mass bound to the hydrogel ($m_{FDH,immo}$) relative to the total enzyme mass initially added to the solution. The enzyme mass was calculated from a mass balance of the supernatant protein concentration measured by the Bradford Assay ($m_{FDH,0}$).

$$Y_{immo} = \frac{m_{FDH,immo}}{m_{FDH,0}} \cdot 100\% \tag{6}$$

The enzyme loading (E) corresponded to the percentage of mass of immobilized enzymes per dry mass of hydrogel. The dry mass of the hydrogel is the reciprocal of the degree of swelling calculated in eq 1 ($m_{carrier,dry}$).

$$E = \frac{m_{FDH,immo}}{m_{carrier,dry}} \tag{7}$$

The activity yield (Y_{EA}) was calculated as the percentage of the specific activity of immobilized enzymes ($EA_{FDH,immo}$) to that of the free enzyme ($EA_{FDH,free}$), reflecting the retained catalytic activity after immobilization. The mass amounts of the enzyme were the same for the activity assay with immobilized enzyme and with free enzyme.

$$Y_{EA} = \frac{EA_{FDH,immo}}{EA_{FDH,free}} \cdot 100\% \tag{8}$$

The specific activity of the immobilized enzymes was determined as described in the section *FDH Activity Assay*. The specific activity of the free enzyme was calculated from the initial NADH synthesis rate in 50 mM potassium phosphate buffer with pH 8 containing 1 mM NAD^+ and 200 mM HCOONa normalized to the mass of enzyme added.

Enzyme leaching was quantified as the percentage of enzyme mass released into the reaction solution during the reaction ($m_{FDH,sol}$) per initial enzyme mass immobilized on the carrier $m_{FDH,immo}$.

$$Leaching = \frac{m_{FDH,sol}}{m_{FDH,immo}} \cdot 100\% \tag{9}$$

Determination of Hydrogel Morphology

For lyophilization, the hydrogels were flash-frozen in liquid nitrogen and then freeze-dried at 0.030 mbar for 24 h. The dried hydrogels were cut and mounted on an scanning electron microscopy (SEM) sample holder using double-sided tape, with the internal structure oriented upward. Each sample was sputtered with gold at 24 °C and a current of 42 mA for 60 s under argon vacuum using the SCD 050 sputter Coater (BAL-TEC AG; Balzers, Liechtenstein). SEM images were taken with the Supra 55VP (Carl Zeiss AG, Oberkochen, Germany) SEM with a field emission cathode and a GEMINI column.

RESULTS AND DISCUSSION

This study characterizes the immobilization of enzymes onto stimuli-responsive polymer carriers, aiming to protect inherently sensitive enzymes from harsh conditions. To this end, various polymer formulations with distinct responsive behaviors as well as different immobilization techniques are evaluated to establish optimal immobilization protocols. This study marks an initial step toward utilizing these materials as biocatalyst carriers in smart bioreactors. The study first characterizes the material and responsive properties of the hydrogels, and then analyzes the hydrogels as enzymatic support matrices.

Material Properties of Smart Carriers

The hydrogel formulations analyzed in this study can be categorized as pH-responsive, temperature-responsive, and dual-responsive, exhibiting both pH and temperature sensitivity. The temperature responsiveness arises from the LCST of the NIPAM monomer, whereas the pH responsiveness of the respective formulations is attributed to the (de)protonation of carboxylic acid groups present in the itaconic acid monomer.

Comparing the swelling behavior and mechanical properties of the hydrogels, the greatest degree of swelling was observed in p(NIPAM-*co*-IA), followed by pure pNIPAM, with p(HEMA-*co*-IA) exhibiting the lowest swelling (Figure 1). The highest elastic modulus was measured for p(HEMA-*co*-IA), indicating the highest rigidity of the polymer network. This behavior can be attributed to differences in polymer composition and network architecture, which influence chain rigidity and the effective cross-link density of the gels. These structural properties impact the swelling behavior, resulting in

https://doi.org/10.1021/acs.iecr.6c00961
Ind. Eng. Chem. Res. XXXX, XXX, XXX−XXX

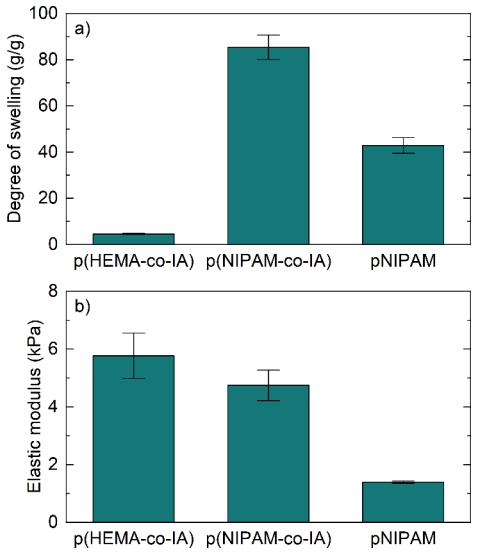

Figure 1. Degree of swelling (a) and elastic modulus (b) comparing p(HEMA-*co*-IA), p(NIPAM-*co*-IA), and pNIPAM at 25 °C in distilled water. Data represent mean ± standard deviation (n = 3).

lower water uptake and higher stiffness for p(HEMA-*co*-IA) compared to the other formulations. In contrast, pNIPAM exhibited the lowest elastic modulus, reflecting a softer polymer network. Among the three materials, the pH-responsive p(HEMA-*co*-IA) formulation also demonstrated the highest stability across all experiments.

In comparison to the study by Milašinović et al.,[21] a significantly larger swelling capacity for p(NIPAM-*co*-IA) and for pNIPAM by the factor of 3.4 was obtained in this work. This increase can be attributed to differences in the synthesis procedure and the type of radical starters used in the polymerization. Nevertheless, the overall trend in swelling behavior remains consistent with that reported by Milašinović et al.[21]

Differences among the gel formulations can be observed not only in swelling but also in their pore morphologies, which influence their suitability for enzyme immobilization. However, it should be noted that the SEM analysis reflects only the structure of freeze-dried gels. Consequently, no definitive conclusions can be drawn regarding the pore structure in the hydrated (wet) state; instead, only general morphological features can be compared. The pH-responsive p(HEMA-*co*-IA) gel can be characterized by a dense, aggregated, cluster-like morphology. In comparison, the pNIPAM-containing formulations exhibit a more open porous morphology (Figure 2). The pure pNIPAM formulation is characterized by smaller, comb-like pore morphologies, whereas in the dual-responsive p(NIPAM-*co*-IA) formulation larger and less regular pore structures can be observed. As the dual-responsive formulation consists predominantly of pNIPAM (90 mol%), the pore morphology is therefore primarily dominated by the pNIPAM component.

Considering the pore morphologies, the rough, cluster-like structure of p(HEMA-*co*-IA) could in principle provide a higher surface area for enzyme immobilization. However, its denser network compared to p(NIPAM-*co*-IA) gels limits the accessible surface area. Furthermore, smaller pores increase diffusion limitations and reduce mass transport in the gels. During the immobilization step, this can subsequently result in lower enzyme loading, and after immobilization, in diminished enzyme activity.[1] Nevertheless, as all pore sizes are within the macroporous range compared to enzymes, which are in the nanoscale, diffusion limitations are expected to be less pronounced, suggesting that the observed differences in enzyme loading and activity are primarily dominated by enzyme-polymer interactions rather than effects caused by pore-sizes.

Responsive Properties of Smart Carriers

In addition to their distinct swelling capacities, the hydrogel formulations exhibit responsiveness to different external stimuli. The presence of carboxylic acid groups in itaconic acid imparts pH-responsiveness, while the lower critical solution temperature (LCST) of NIPAM confers temperature-responsiveness to the resulting polymer matrices as described in the introduction. These effects are clearly demonstrated in the swelling analyses (Figure 3).

Among the tested formulations, distinct stimulus-responsive behaviors were observed. p(HEMA-*co*-IA) exhibits the strongest pH-responsiveness, whereas pNIPAM hydrogels show no pH-response but display the most pronounced temperature responsiveness. In contrast, pNIPAM gels demonstrate noticeable temperature-responsiveness, followed by p(NIPAM-*co*-IA), whereas p(HEMA-*co*-IA) shows no temperature response. For p(NIPAM-*co*-IA), dual-responsive behavior could be confirmed.[21] While temperature-induced shrinkage appeared less prominent in the dual-responsive formulation compared to the corresponding single-responsive system of pNIPAM hydrogels, pH-induced shrinkage was comparable to that of p(HEMA-*co*-IA) hydrogels as a single-responsive system. This behavior can be attributed to the monomer fractions of itaconic acid (10 mol%, Table 1) within the gel formulations. The itaconic acid content, which accounts for the pH-responsivity of the hydrogels, is identical in p(HEMA-*co*-IA) and p(NIPAM-*co*-IA), whereas the fraction of the temperature-responsive monomer NIPAM is lower in

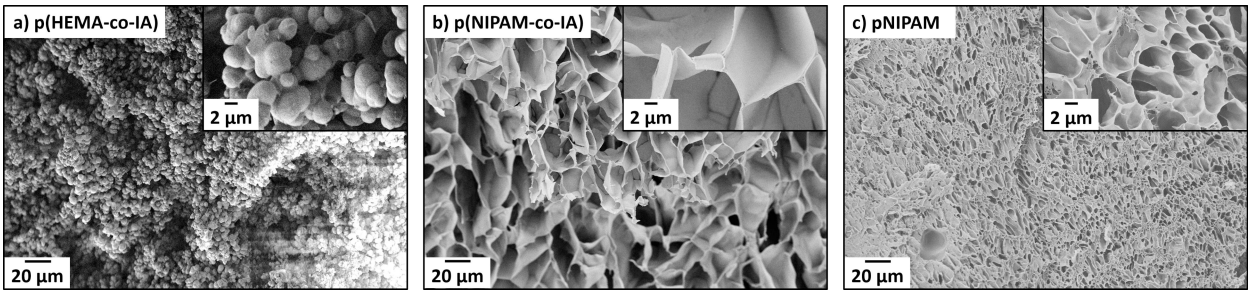

Figure 2. SEM micrographs of freeze-dried p(HEMA-*co*-IA) (a), p(NIPAM-*co*-IA) (b), and pNIPAM (c) gels.

https://doi.org/10.1021/acs.iecr.6c00961
Ind. Eng. Chem. Res. XXXX, XXX, XXX−XXX

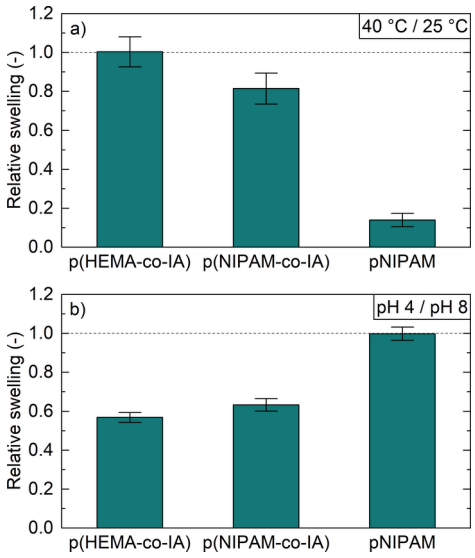

Figure 3. Relative swelling of hydrogels comparing p(HEMA-*co*-IA), p(NIPAM-*co*-IA), pNIPAM. The temperature-induced swelling represents the swelling at 40 °C relative to 25 °C (a) and the pH-induced swelling pH 4 relative to pH 8 (b). Data represent mean ± standard deviation (n = 3).

p(NIPAM-*co*-IA) hydrogels than in pure pNIPAM hydrogels, resulting in a reduced thermoresponse.

Based on these findings, it can be concluded that all formulations exhibit significant stimulus-responsive behavior and, due to their porous structure, are expected to be suitable as self-regulating, adaptable carrier materials. The next step involves evaluating their applicability as enzyme carriers, particularly for supporting and protecting inherently sensitive enzymes. To this end, the immobilization of FDH is investigated in the following chapter.

3.3. Characterization of Enzyme Immobilization on Smart Materials

To characterize the immobilization method, a series of parameters were investigated including monomer composition, size of the hydrogel cylinders, and the immobilization method (Table 2).

Immobilization Yield. The adsorptive immobilization yield across all monolithic hydrogels remained relatively constant between 32.4 ± 8.7% for pNIPAM and 41.8 ± 14.1% for p(HEMA-*co*-IA) (Figure 4 a). Adsorptive immobilization is primarily governed by the surface interactions between the enzyme and the polymer surface, as well as by the porous structure of the material. Although the carriers exhibit distinctly different pore morphologies, all are characterized by macroporous structures (Figure 2). Given the similar immobilization yield across formulations, the main impacting factor is the presence of macropores rather than the specific morphological arrangement.

In comparison to adsorption, covalent immobilization over 24 h slightly improved the immobilization yield for p(HEMA-*co*-IA) and p(NIPAM-*co*-IA), although the improvement was not statistically significant given the data variability. In the case of immobilization onto hydrogel particles, significantly lower yields were obtained for pNIPAM compared to the other formulations (Figure 4 b). This may be due to the absence of functional groups in pNIPAM that can react with the EDC/NHS functionalization. To the best of our knowledge, no reports describing covalent binding of enzymes to pure pNIPAM were found. Instead, comonomers containing carboxyl groups are routinely incorporated into pNIPAM gels to enable covalent enzyme immobilization.[30,31] In this study, carboxylic groups were introduced into p(NIPAM-*co*-IA) gels by copolymerizing itaconic acid with the NIPAM monomer as described in the Hydrogel Synthesis and Characterization section.

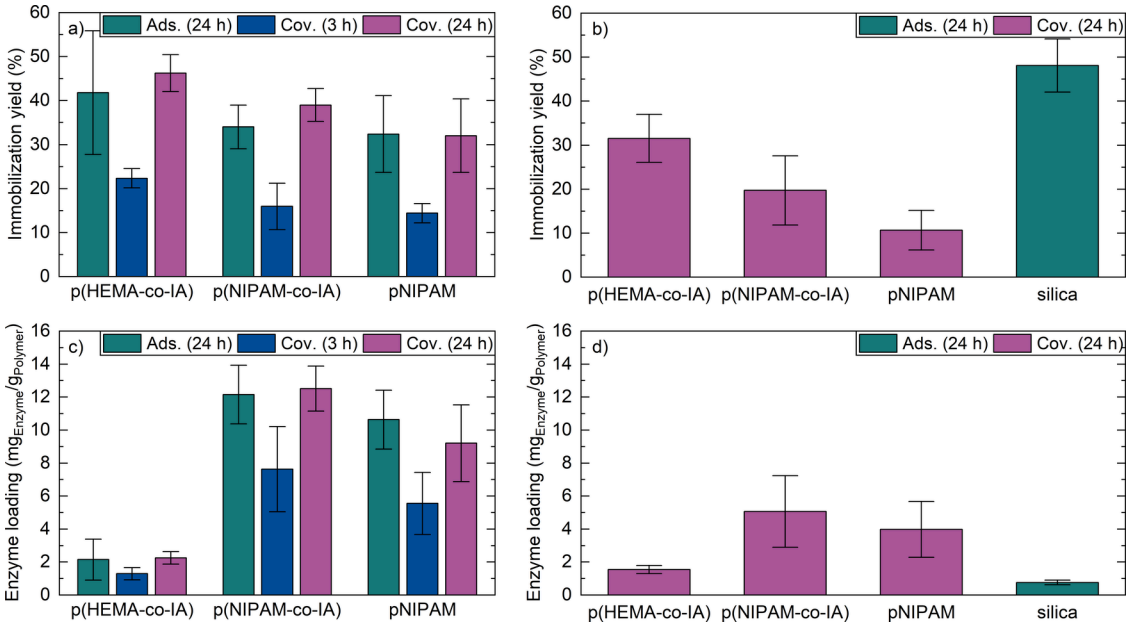

Figure 4. Immobilization yield (a, b) and enzyme loading (c, d) of formate dehydrogenase on monolithic hydrogels (a, c) and particle hydrogels (b, d) via adsorption (24 h, teal), covalent binding (3 h, dark blue), and covalent binding (24 h, pink). Data represent mean ± standard deviation (n = 3) for p(HEMA-*co*-IA), p(NIPAM-*co*-IA), and pNIPAM hydrogels.

https://doi.org/10.1021/acs.iecr.6c00961
Ind. Eng. Chem. Res. XXXX, XXX, XXX−XXX

The lowest immobilization yield on the monolithic hydrogels was the covalent binding for 3 h across all three hydrogels. Prolonged contact between the activated hydrogel surface and the enzyme likely enhances attachment by allowing extended interaction with available functional groups. Furthermore, the diffusion limitation of the enzyme into the gel matrix is significantly more pronounced for shorter exposure times. Comparing the monolithic hydrogels (Figure 4 a) and particle hydrogels (Figure 4 b), the overall immobilization yield trend between hydrogel compositions is analogous. The lower immobilization yield observed for particles compared with hydrogel monoliths may arise from stronger washing-out of loosely bound enzyme. Particles have a higher external surface-to-volume ratio and shorter diffusion paths, which, under flow or agitation conditions, can facilitate loss of enzyme during the wash, thereby reducing the apparent immobilization yield. The immobilization yield on the nonresponsive enzyme carrier (silica) was the highest among the carriers likely due to the mesoporous structure of the silica gels compared to the macropores of the hydrogels.

Enzyme Loading. While immobilization yield shows the efficiency of enzyme binding based on the enzyme amount added initially, enzyme loading represents the relative amount of enzyme immobilized per unit carrier mass as a metric for evaluating carrier utilization efficiency. The highest enzyme loading was observed for p(NIPAM-*co*-IA), closely followed by pNIPAM, with p(HEMA-*co*-IA) showing the lowest enzyme loading regardless of the immobilization method (Figure 4 c, d). These results align with the degree of swelling shown in Figure 1, since swelling degree inversely relates to the carrier's dry mass. Hydrogels with a lower degree of swelling, such as p(HEMA-*co*-IA), contain more polymer per unit wet volume and thus exhibit a higher dry mass. Comparing the three formulations, p(HEMA-*co*-IA) exhibits the highest network density and therefore the lowest degree of swelling (see Figure 1). Consequently, gels such as p(HEMA-*co*-IA) contain more polymer per unit wet volume and thus exhibit a higher dry mass. When quantifying enzyme immobilization in terms of the dry mass of the carrier (i.e., loading), hydrogels with higher dry mass will exhibit lower enzyme loading per unit mass, assuming a constant absolute amount of enzyme is immobilized. Consequently, the observed differences in loading primarily reflect differences in polymer chemistry and swelling behavior rather than superior binding efficiency. Reducing the monolith dimensions to the particle size significantly affected immobilization yield (Figure 4 b). For polymer-based monoliths, yields decreased compared to the larger structures, while silica particles exhibited the highest immobilization yield under adsorption conditions. This trend can be attributed to the increased surface-to-volume ratio and rapid adsorption kinetics of silica at smaller length scales. However, when enzyme loading was considered (Figure 4 d), silica displayed the lowest performance by a wide margin, demonstrating that high immobilization yield does not necessarily translate into efficient enzyme utilization per unit mass of carrier.

These findings suggest that responsive polymer carriers can indeed serve as effective alternatives to nonresponsive carriers when enzyme mass efficiency is prioritized. Furthermore, the hydrogel formulations could be tailored in future studies to higher polarities or other chemical properties to enhance immobilization performance for specific enzymes. The consistent superiority of p(NIPAM-*co*-IA) in terms of loading across both monolith sizes highlights that carrier chemistry, rather than geometry, is the dominant factor controlling enzyme density. Enzyme loading is typically assessed alongside the residual catalytic activity after immobilization. Lower enzyme loadings often promote greater substrate accessibility to the active sites, by reducing diffusional barriers such as pore blockage and minimizing steric crowding among immobilized enzyme molecules. Conversely, higher enzyme loading per gram of carrier increases the number of available catalytic sites, potentially enhancing bulk catalytic activity.[32] This fundamental trade-off necessitates optimization based on application requirements, whether the priority is substrate accessibility (lower loading) or maximum catalytic capacity (higher loading).

3.3.3. Activity Yield. One of the most important parameters in biocatalytic processes is the enzyme activity after immobilization. Accordingly, the activity yield of the enzyme was determined for each hydrogel and immobilization approach (Figure 5 a). The activity yield of the enzyme for all

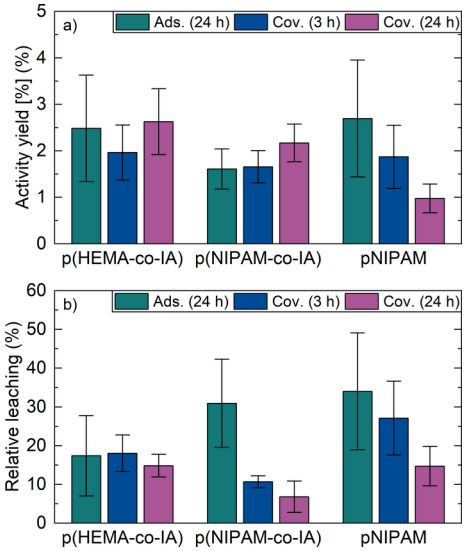

Figure 5. Activity yield (Conditions: 200 mM NaCOOH, 1 mM NAD^+ in 50 mM potassium phosphate buffer pH 8 at 25 °C) (a) and relative enzyme leaching (b) of FDH immobilized on monolithic hydrogels via adsorption (24 h, teal), covalent binding (3 h, blue), and covalent binding (24 h, pink). Data represent mean ± standard deviation (n = 3) for p(HEMA-*co*-IA), p(NIPAM-*co*-IA), and pNIPAM hydrogels.

gels was low, ranging between 0.97 ± 0.31% (pNIPAM with 24 h covalent immobilization) and 2.69 ± 1.25% (pNIPAM with adsorption). However, these low apparent activity values do not reflect loss of catalytic activity during immobilization, but rather diffusion-limited kinetics in the batch assay. In macroporous hydrogels of large dimensions, substrate diffusion from bulk solution to the interior becomes rate-limiting, with local substrate concentrations in the hydrogel core significantly lower than bulk conditions.[33] Consequently, only enzymes at the outer surface encounter the full bulk substrate concentration, while interior enzymes operate at reduced concentrations. Thus, the measured activity represents an apparent activity governed by the interplay of enzyme kinetics and substrate diffusion through the macroporous network, rather than intrinsic enzyme inactivation. This can be addressed in part by establishing a high convective flux on the immobilizates. Additionally, immobilization can change the

https://doi.org/10.1021/acs.iecr.6c00961
Ind. Eng. Chem. Res. XXXX, XXX, XXX−XXX

enzyme structure, thus leading also to a change in activity, and a reduction of the immobilized activity compared to free enzyme activity.[32] Shiroya et al. immobilized trypsin onto pNIPAM gels, and determined activity yields between 8 and 17%, which is within the range of the obtained results in this study.[31]

The duration of the covalent binding appears to have no significant effect on the activity yield of the hydrogels. The similar activity yields across 3 and 24 h covalent coupling suggest that intrinsic enzyme catalytic capacity is largely unaffected by covalent binding duration. The additional enzyme bound at 24 h is also subject to diffusion limitation and thus contributes little additional measurable activity in the batch format. Overall, comparable results could be achieved using both the adsorptive and the prolonged covalent binding procedure. For pNIPAM carriers, adsorption yielded slightly higher apparent activity than covalent coupling, though not significantly. As pNIPAM does not possess functional groups suitable for covalent attachment, the observed difference is primarily attributable to the immobilization conditions rather than an inherent advantage of the method. We propose that EDC/NHS coupling reagents remained largely unreacted and were therefore not fully removed during washing, in contrast to hydrogels containing itaconic acid, where functional groups consume the reagents. The unwashed coupling agents could, therefore, have negative effects on enzyme activity. To assess intrinsic enzyme activity and distinguish immobilization-induced deactivation from diffusion limitation, Part B of this paper uses a flow reactor and the reduced particle sizes to minimize mass transfer resistance.[34]

Enzyme Leaching. To further evaluate the immobilization, the relative leaching of the enzyme for each hydrogel was investigated. Due to the weaker binding mechanism, the highest leaching was expected for adsorptive immobilization. This trend was generally observed across formulations, although differences were not statistically significant in all cases. Enzyme leaching in the case of covalent binding is due to unspecific binding of enzymes to the hydrogel through ad- and absorption of the enzyme into the hydrogel matrix itself. Comparing the hydrogel formulations, p(HEMA-*co*-IA) exhibited relatively low enzyme leaching for all immobilization approaches, with only approximately 20% of the enzyme leached even after adsorptive immobilization (corresponding to ∼80% retention, Figure 5 b). This robust retention may be attributed to the cluster-like morphology of HEMA-*co*-IA, which provides a larger surface area for enzyme-polymer interactions, and to the higher polarity of the material, arising from the monomer composition, both factors that enhance electrostatic and hydrophilic interactions with enzymes. In contrast, higher enzyme loss was determined for p(NIPAM-*co*-IA) and pNIPAM when using the adsorptive method compared to covalent binding. In these systems, a higher incubation time for covalent binding was advantageous for reducing enzyme loss. Overall, the responsive hydrogels are promising as smart enzyme carriers, combining reasonable immobilization yields, and high enzyme loading density with strong potential in continuous-flow reactors where improved substrate accessibility can overcome diffusion limitations.

CONCLUSION

The overall aim of this work was to evaluate stimuli-responsive hydrogels as smart carriers, comparing distinct methods and conditions to establish an optimized protocol for enhanced biocatalytic performance. A systematic characterization of three responsive hydrogel formulations across multiple immobilization and operational parameters revealed key findings.

All three hydrogel formulations displayed the expected stimuli-responsive behavior, with p(HEMA-*co*-IA) exhibiting pronounced pH-responsiveness, pNIPAM showing strong temperature-responsiveness, and p(NIPAM-*co*-IA) demonstrating dual pH- and temperature-responsiveness. High immobilization yields were achieved across all formulations, particularly when longer immobilization times were employed, due to extended diffusion times and increased interactions between hydrogel and enzyme. Notably, little difference in immobilization yield was observed between adsorption and covalent binding after 24 h, indicating that both methods are similarly effective for initial enzyme capture.

Enzyme loading is determined primarily by the dry mass of the carrier rather than the immobilization method, emphasizing the critical importance of carrier chemistry and swelling behavior in governing loading capacity. Batch assay activity yields primarily reflect substrate diffusion limitations rather than enzyme inactivation during immobilization, as indicated by consistent activity across methods and immobilization times. For p(NIPAM-*co*-IA) and pNIPAM, 24 h covalent attachment reduces enzyme leaching compared to adsorption, confirming covalent coupling as the superior strategy for long-term carrier stability.

The combination of adequate immobilization efficiency, substantial enzyme loading capacity, mechanical properties, and tunable responsiveness to external stimuli positions these hydrogels as promising materials for biocatalytic applications. The stimulus-responsive behavior enables external control over enzyme activity and carrier properties, offering potential advantages for protecting sensitive enzymes from unfavorable process conditions. Part B[34] of this work employs a continuous-flow reactor to demonstrate that these responsive carriers can overcome the diffusion limitations observed in batch assays and achieve improved catalytic performance.[34] These characteristics make the hydrogels especially attractive for practical applications involving cofactor regeneration and other biocatalytic processes. Moreover, these smart carriers provide enzyme resilience and stability, which are critical for practical implementation in smart bioreactor systems where stimuli-responsive control can be leveraged to enhance cofactor reuse and process efficiency.

ASSOCIATED CONTENT

Supporting Information

The Supporting Information is available free of charge at https://pubs.acs.org/doi/10.1021/acs.iecr.6c00961.

Numerical values and tabulated data for all analyses presented in the manuscript (PDF)

AUTHOR INFORMATION

Corresponding Author

Andreas Liese − *Institute of Technical Biocatalysis, Hamburg University of Technology, 21073 Hamburg, Germany; United Nations University Hub on Engineering to Face Climate Change at the Hamburg University of Technology, United Nations University Institute for Water, Environment and Health (UNU-INWEH), 21073 Hamburg, Germany;* orcid.org/0000-0002-4867-9935; Email: liese@tuhh.de

https://doi.org/10.1021/acs.iecr.6c00961
Ind. Eng. Chem. Res. XXXX, XXX, XXX−XXX

Authors

Kayla Reata Dittmer − *Institute of Technical Biocatalysis, Hamburg University of Technology, 21073 Hamburg, Germany; United Nations University Hub on Engineering to Face Climate Change at the Hamburg University of Technology, United Nations University Institute for Water, Environment and Health (UNU-INWEH), 21073 Hamburg, Germany*

Kathrin Marina Eckert − *Institute of Thermal Separation Processes, Hamburg University of Technology, 21073 Hamburg, Germany; United Nations University Hub on Engineering to Face Climate Change at the Hamburg University of Technology, United Nations University Institute for Water, Environment and Health (UNU-INWEH), 21073 Hamburg, Germany;* orcid.org/0000-0002-8454-4886

Sherliana Setiawan − *Institute of Technical Biocatalysis, Hamburg University of Technology, 21073 Hamburg, Germany; United Nations University Hub on Engineering to Face Climate Change at the Hamburg University of Technology, United Nations University Institute for Water, Environment and Health (UNU-INWEH), 21073 Hamburg, Germany*

Patrick André Kißling − *Institute of Chemical Reaction Engineering, Hamburg University of Technology, 21073 Hamburg, Germany*

Daniel Ohde − *Institute of Technical Biocatalysis, Hamburg University of Technology, 21073 Hamburg, Germany; United Nations University Hub on Engineering to Face Climate Change at the Hamburg University of Technology, United Nations University Institute for Water, Environment and Health (UNU-INWEH), 21073 Hamburg, Germany*

Irina Smirnova − *Institute of Thermal Separation Processes, Hamburg University of Technology, 21073 Hamburg, Germany; United Nations University Hub on Engineering to Face Climate Change at the Hamburg University of Technology, United Nations University Institute for Water, Environment and Health (UNU-INWEH), 21073 Hamburg, Germany;* orcid.org/0000-0003-4503-4039

Complete contact information is available at: https://pubs.acs.org/10.1021/acs.iecr.6c00961

Notes

The authors declare no competing financial interest.

■ ACKNOWLEDGMENTS

This project is funded by the Deutsche Forschungsgemeinschaft (DFG, German Research Foundation) − SFB 1615 − 503850735.

■ REFERENCES

(1) Liese, A.; Hilterhaus, L. Evaluation of immobilized enzymes for industrial applications. *Chem. Soc. Rev.* **2013**, *42*, 6236.

(2) Cumana, S.; Simons, J.; Liese, A.; Hilterhaus, L.; Smirnova, I. Immobilization of glucose 6-phosphate dehydrogenase in silica-based hydrogels: A comparative study. *Journal of Molecular Catalysis B: Enzymatic* **2013**, *85*−*86*, 220−228.

(3) Rouf, S.; Greish, Y. E.; Van der Bruggen, B.; Al Zuhair, S. CO_2 hydrogenation to formate by immobilized formate dehydrogenase: Challenges and opportunities. *Int. J. Hydrogen Energy* **2025**, *142*, 1067−1074.

(4) Schlager, S.; Dibenedetto, A.; Aresta, M.; Apaydin, D. H.; Dumitru, L. M.; Neugebauer, H.; Sariciftci, N. S. Biocatalytic and Bioelectrocatalytic Approaches for the Reduction of Carbon Dioxide using Enzymes. *Energy Technology* **2017**, *5*, 812−821.

(5) Romero, M. R.; Wolfel, A.; Igarzabal, C. I. A. Smart valve: Polymer actuator to moisture soil control. *Sens. Actuators, B* **2016**, *234*, 53−62.

(6) Bajpai, A. K.; Shukla, S.; Bhanu, S.; Kankane, S. Responsive Polymers in Controlled Drug Delivery. *Prog. Polym. Sci.* **2008**, *33*, 1088−1118.

(7) Hydrogel Sensors and Actuators: Engineering and Technology; Gerlach, G., Arndt, K.-F., Eds.; *Springer Series on Chemical Sensors and Biosensors*, Vol. *6*; Springer Berlin Heidelberg: Berlin, Heidelberg, 2010.

(8) Shen, C.; Wang, Y.; Xiao, X.; Yang, R.; Chen, H.; Yuan, P.; Zhang, Y.; Lyu, G.; Shin, J.; Chen, G., et al. Hydrogels for In Vivo Biomedical Applications: Recent Advances and Future Perspectives. *J. Mater. Chem. B* **2026**.*142*386

(9) Nastyshyn, S.; Stetsyshyn, Y.; Raczkowska, J.; Nastishin, Y.; Melnyk, Y.; Panchenko, Y.; Budkowski, A. Temperature-Responsive Polymer Brush Coatings for Advanced Biomedical Applications. *Polymers* **2022**, *14* (19), 4245.

(10) Kocak, G.; Tuncer, C.; Bütün, V. pH-Responsive polymers. *Polym. Chem.* **2017**, *8*, 144−176.

(11) Dübner, M.; Cadarso, V. J.; Gevrek, T. N.; Sanyal, A.; Spencer, N. D.; Padeste, C. Reversible Light-Switching of Enzymatic Activity on Orthogonally Functionalized Polymer Brushes. *ACS Appl. Mater. Interfaces* **2017**, *9*, 9245−9249.

(12) Cirillo, G.; Nicoletta, F. P.; Curcio, M.; Spizzirri, U. G.; Picci, N.; Iemma, F. Enzyme immobilization on smart polymers: *Catalysis on demand*. *React. Funct. Polym.* **2014**, *83*, 62−69.

(13) Cullen, S. P.; Liu, X.; Mandel, I. C.; Himpsel, F. J.; Gopalan, P. Polymeric Brushes as Functional Templates for Immobilizing Ribonuclease A: Study of Binding Kinetics and Activity. *Langmuir* **2008**, *24*, 913−920.

(14) González-Sáiz, J. M.; Pizarro, C. Polyacrylamide gels as support for enzyme immobilization by entrapment. Effect of polyelectrolyte carrier, pH and temperature on enzyme action and kinetics parameters. *Eur. Polym. J.* **2001**, *37*, 435−444.

(15) Eixenberger, D.; Kumar, A.; Klinger, S.; Scharnagl, N.; Dawood, A. W. H.; Liese, A. Polymer-Grafted 3D-Printed Material for Enzyme Immobilization—Designing a Smart Enzyme Carrier. *Catalysts* **2023**, *13* (7), 1130.

(16) Koenig, M.; Bittrich, E.; König, U.; Rajeev, B. L.; Müller, M.; Eichhorn, K.-J.; Thomas, S.; Stamm, M.; Uhlmann, P. Adsorption of enzymes to stimuli-responsive polymer brushes: Influence of brush conformation on adsorbed amount and biocatalytic activity. *Colloids Surf., B* **2016**, *146*, 737−745.

(17) Nagel, B.; Warsinke, A.; Katterle, M. Enzyme Activity Control by Responsive Redoxpolymers. *Langmuir* **2007**, *23*, 6807−6811.

(18) Tam, T. K.; Zhou, J.; Pita, M.; Ornatska, M.; Minko, S.; Katz, E. Biochemically Controlled Bioelectrocatalytic Interface. *J. Am. Chem. Soc.* **2008**, *130*, 10888−10889.

(19) Poschlad, K.; Enders, S. Thermodynamics of aqueous solutions containing poly (N-isopropylacrylamide). *J. Chem. Thermodyn.* **2011**, *43*, 262−269.

(20) Chen, Q.; Li, S.; Feng, Z.; Wang, M.; Cai, C.; Wang, J.; Zhang, L. Poly(2-(diethylamino)ethyl methacrylate)-based, pH-responsive, copolymeric mixed micelles for targeting anticancer drug control release. *Int. J. Nanomed.* **2017**, *12*, 6857−6870.

(21) Milašinović, N.; Milosavljević, N.; Filipović, J.; Kneževič-Jugović, Z.; Krušić, M. K. Synthesis, characterization and application of poly(*N*-isopropylacrylamide-*co*-itaconic acid) hydrogels as supports for lipase immobilization. *React. Funct. Polym.* **2010**, *70*, 807−814.

(22) Claaßen, C.; Gerlach, T.; Rother, D. Stimulus-Responsive Regulation of Enzyme Activity for One-Step and Multi-Step Syntheses. *Advanced Synthesis & Catalysis* **2019**, *361*, 2387−2401.

(23) Nöth, M.; Gau, E.; Jung, F.; Davari, M. D.; El-Awaad, I.; Pich, A.; Schwaneberg, U. Biocatalytic microgels (μ -Gelzymes): synthesis, concepts, and emerging applications. *Green Chem.* **2020**, *22*, 8183−8209.

(24) Dubey, N. C.; Gaur, D.; Tripathi, B. P. Responsive microgels and microgel assemblies in biocatalytic applications. *J. Polym. Sci.* **2023**, *61*, 1730−1748.
(25) Bradford, M. M. A rapid and sensitive method for the quantitation of microgram quantities of protein utilizing the principle of protein-dye binding. *Anal. Biochem.* **1976**, *72*, 248−254.
(26) Serial, M. R.; Schmidt, L.; Adrian, M.; Brauckmann, G.; Benders, S.; Bueschler, V.; Liese, A.; Penn, A. A novel method for quantifying enzyme immobilization in porous carriers using simple NMR relaxometry. *Biochemical Engineering Journal* **2026**, *225*, 109909.
(27) Wang, X.; Kim, S. B.; Khang, D.; Kim, H.-H.; Kim, C.-J. Optimization and characterization of covalent immobilization of glucose oxidase for bioelectronic devices. *Biochemical Engineering Journal* **2016**, *112*, 20−31.
(28) Ispas, C.; Sokolov, I.; Andreescu, S. Enzyme-functionalized mesoporous silica for bioanalytical applications. *Anal. Bioanal. Chem.* **2009**, *393*, 543−554.
(29) Lampinen, J.; Raitio, M.; Perälä, A.; Oranen, H.; Harinen, R.-R. *Microplate Based Pathlength Correction Method for Photometric DNA Quantification Assay*; Thermo Fisher Scientific.
(30) Rauer, S. B.; Stüwe, L.; Steinbeck, L.; De Toledo, M. A. S.; Fischer, G.; Wennemaring, S.; Marschick, J.; Koschmieder, S.; Wessling, M.; Linkhorst, J. Cell Adhesion and Local Cytokine Control on Protein-Functionalized PNIPAM-co-AAc Hydrogel Microcarriers. *Small* **2025**, *21*, 2404183.
(31) Shiroya, T.; Tamura, N.; Yasui, M.; Fujimoto, K.; Kawaguchi, H. Enzyme immobilization on thermosensitive hydrogel microspheres. *Colloids Surf., B* **1995**, *4*, 267−274.
(32) Bolivar, J. M.; Woodley, J. M.; Fernandez-Lafuente, R. Is enzyme immobilization a mature discipline? Some critical considerations to capitalize on the benefits of immobilization. *Chem. Soc. Rev.* **2022**, *51*, 6251−6290.
(33) Xiu, G.-h.; Jiang, L.; Li, P. Mass-Transfer Limitations for Immobilized Enzyme-Catalyzed Kinetic Resolution of Racemate in a Batch Reactor. *Ind. Eng. Chem. Res.* **2000**, *39*, 4054−4062.
(34) Eckert, K. M.; Dittmer, K. R.; Setiawan, S.; Ohde, D.; Liese, A.; Smirnova, I. Enzyme Immobilization on Stimuli-Responsive Hydrogels − Part B. Impact of Carrier Responsiveness on Reactor Performance. *Ind. Eng. Chem. Res.* (**applicable**).**2026** DOI: 10.1021/acs.iecr.6c00960

https://doi.org/10.1021/acs.iecr.6c00961
Ind. Eng. Chem. Res. XXXX, XXX, XXX−XXX